Femtosecond Fluorescence Dynamics Imaging Using a Fluorescence Up-Conversion Microscope

Tatsuya Fujino,† Takuya Fujima, and Tahei Tahara*

Molecular Spectroscopy Laboratory, RIKEN (The Institute of Physical and Chemical Research), 2-1 Hirosawa, Wako 351-0198, Japan

Received: March 30, 2005; In Final Form: June 18, 2005

Femtosecond fluorescence dynamics imaging microscopy was performed. Femtosecond fluorescence dynamics images were constructed based on the "mean" fluorescence decay or rise time constants that were evaluated by the time-resolved intensity sampling using a fluorescence up-conversion microscope. This dynamics imaging microscopy was carried out for the organic microcrystals α-perylene and tetracene-doped anthracene microcrystal, and ultrafast dynamics in the organic microcrystals were clearly imaged in the two-dimensional manner. For the α-perylene microcrystal, the obtained dynamics images showed that the crystal edges exhibited relatively shorter free exciton and the Y-state lifetimes compared to the crystal center, reflecting the higher concentration of defects. For the tetracene-doped anthracene microcrystal, the image was constructed based on the time constant of excitation energy transfer from anthracene to tetracene. By experiments changing the doping ratio of tetracene in anthracene, it was concluded that the inhomogeneity observed in the dynamics image arises from the difference in the local concentration of tetracene in the mixed crystal.

1. Introduction

The combination of fluorescence spectroscopy and microscopy makes it possible to obtain detailed and selective information at microscopic levels. In biological studies, for example, a specific organelle in a cell can be selectively stained by fluorescent probes, and it can be identified in fluorescence images. However, fluorescence microscopy often suffers from problems such as photobleaching, probe concentration variation, and scattering artifacts when the image is made based only on the fluorescence intensity. Such drawbacks can be excluded by adopting a fluorescence lifetime as another measure. Furthermore, it becomes possible to distinguish between fluorescence dyes that have a similar spectral property by measuring fluorescence lifetimes. Therefore, the fluorescence lifetime imaging microscopy (FLIM) attracts interest because it can provide additional information about the local and chemical properties in the microscopic samples.

The time-resolved techniques used for fluorescence lifetime imaging microscopy (FLIM) were usually based on the time-gating system,[1,2] time-correlated single photon counting,[3−7] or streak camera.[8,9] Therefore, the time resolution of the FLIM system depends on the detection system, and it is limited to several tens of picoseconds or nanoseconds time regimes. For the FLIM measurements, such time resolution is often considered to be enough because the fluorescence lifetime is as long as nanoseconds in usual cases. However, fluorescence dynamics in the femtosecond or the picosecond time region gives us fruitful information about the molecular dynamics such as solvation, energy transfer, and rotation diffusion. Thus, the imaging microscopy has the potential to provide much more information if we can observe the fluorescence in the microscopic region with a higher time resolution.

Recently, we have developed a time-resolved fluorescence microscope (femtosecond fluorescence up-conversion microscope) that simultaneously achieves diffraction-limited space resolution and femtosecond time resolution.[10,11] The high time resolution of this time-resolved microscope was realized by the up-conversion technique: the fluorescence from the sample is mixed with a femtosecond gate pulse in an optical nonlinear crystal, and the frequency up-converted fluorescence is detected.[12,13] Since the intensity of the up-converted fluorescence is proportional to the intensity of the fluorescence that is temporally overlapped with the femtosecond gate pulse, femtosecond time resolution was readily achieved. The fluorescence up-conversion microscope enabled us to measure the ultrafast dynamics of microscopic samples. In fact, we have investigated the ultrafast exciton dynamics in organic microcrystals,[10] as well as the rotation and vibrational cooling process of dye molecules in micrometer-sized droplets in liquids.[11]

In this paper, we report the application of the femtosecond fluorescence up-conversion microscope to the imaging measurements (femtosecond fluorescence dynamics imaging). The fluorescence dynamics images were obtained by scanning the *XY* translational sample stage and by intensity sampling of the time-resolved up-converted fluorescence. The imaging based on ultrafast fluorescence dynamics was demonstrated for organic microcrystals, α-perylene and tetracene-doped anthracene microcrystal, and the position dependence of the picosecond/femtosecond fluorescence dynamics was visualized.

2. Experimental Section

Figure 1 shows the schematic diagram of the apparatus that was used for the femtosecond fluorescence dynamics imaging. The fluorescence up-conversion microscope has been described in detail elsewhere.[11] Briefly, a mode-locked Ti:sapphire laser

* To whom correspondence should be addressed. Phone: +81-48-467-7928. Fax: +81-48-467-4539. E-mail: tahei@riken.jp.

† Current address: Tokyo Metropolitan University, 1-1 Mainami-Osawa, Hachioji-shi 192-0397, Japan.

10.1021/jp0516083 CCC: $30.25
Published on Web 07/21/2005

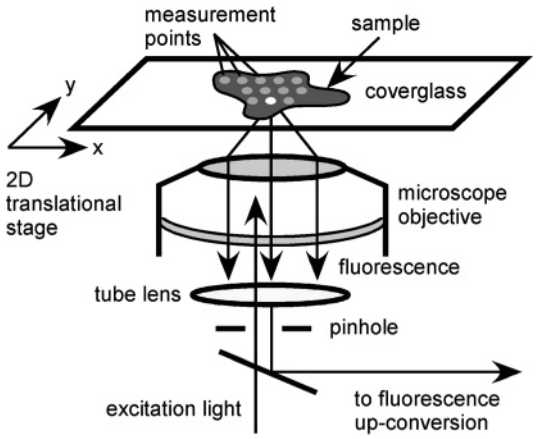

Figure 1. Schematic diagram of the femtosecond fluorescence dynamics imaging microscope.

(Coherent, Mira-900F) that was pumped by an Nd:YVO_4 laser (Coherent, Verdi V-10) provided femtosecond pulses (800 nm, 26 nJ, 110 fs) at a repetition rate of 76 MHz. The second harmonic of the laser output was used as excitation light (400 nm, <12 pJ), and it was introduced into an inverted confocal microscope (Nikon, TE-2000U). The excitation light was focused on the sample by the microscope objective lens (Nikon, CFI Plan Fluor 100×, N.A. 1.3, oil), and the fluorescence from the sample was collected by the same objective lens in the backscattering geometry. The fluorescence was guided to the outside of the microscope through a pinhole that only passes the fluorescence from the focal plane, and it was separated from the excitation light by a dichroic mirror. Then, the fluorescence was frequency up-converted with the time-delayed fundamental laser pulse in a BBO crystal. The up-converted fluorescence was separated by a band-pass filter and a monochromator, and then it was detected by a photon-counting system. The best resolutions of the system were $\Delta t \sim 520$ fs (time), $\Delta XY \sim 340$ nm (transverse), and $\Delta Z \sim 1.1$ μm (axial) for 600-nm fluorescence with a 50-μm pinhole.[11] In the present work, a translational stage (Sigma Koki, BIOS-412T, FC-501G) was implemented in the inverted microscope to realize computer-controlled automatic *XY* scanning. The femtosecond fluorescence dynamics images were obtained by the *XY* scanning of the sample position with the translational stage, and the best translational resolution of the stage was as high as ~10 nm.

In the present work, we made two-dimensional images based on the femtosecond time-resolved fluorescence data measured at each position of the sample. We evaluated the "mean" decay (rise) time of the time-resolved fluorescence at each position to represent the position dependence of the fluorescence dynamics. For the fluorescence decay, the up-converted intensity was sampled at three delay times (Figure 2a), and the mean decay time constant τ was determined by the following equation, assuming a single-exponential decay,

$$\tau = \frac{\Delta T}{\ln((I_{t_1} - I_{BG})/(I_{t_2} - I_{BG}))} \quad (1)$$

where ΔT is the time interval between the two positive delay times, and I_{t_1}, I_{t_2}, and I_{BG} are the up-converted intensities at two positive delay times and at one negative delay time, respectively. For the fluorescence showing an exponential rise (as shown in Figure 2b), the up-converted signal was sampled at four delay times (three positive delay times and one negative delay time), and then the averaged rise time constant τ was

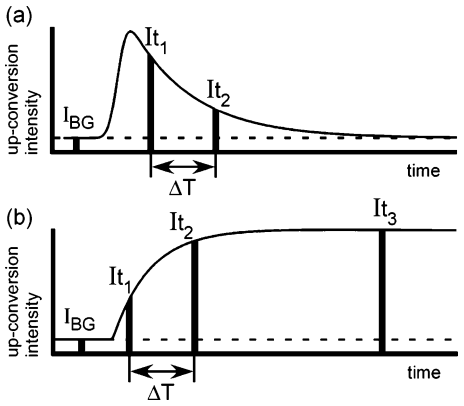

Figure 2. The principle for the intensity sampling of the time-resolved fluorescence. The sample is excited with a femtosecond pulse, after which the fluorescence decay (up-converted intensity) is measured at two different positive delay times and one negative delay time (a). When the fluorescence shows a rise, the intensity of the up-converted fluorescence is measured at three positive delay times and one negative delay time (b).

evaluated by fitting with the following single-exponential function,

$$I(t) - I_{BG} = A\left(1 - \exp\left(-\frac{t}{\tau}\right)\right) \quad (2)$$

where t and A are the fitting parameter. In either case, the heterogeneity of the sample was visualized in a two-dimensional manner on the basis of the τ value evaluated at each sample point.

3. Result and Discussion

3.1. α-Perylene Microcrystal (the exciton relaxation dynamics). Femtosecond fluorescence dynamics imaging was first performed for an organic microcrystal, α-perylene. The α-perylene microcrystal used for the imaging experiment is shown in Figure 3a. The microcrystal was prepared by the recrystallization of a toluene solution of perylene.[14] By the photoexcitation with 400-nm light, the α-perylene exhibits a very broad fluorescence spectrum with an intensity maximum around ~600 nm. The fluorescence in blue region (~480 nm) has been assigned to the emission of the free exciton that is generated with photoexcitation. The free exciton is relaxed to the Y-state and gives fluorescence around ~530 nm. Then the Y-state is relaxed to the E-state that gives broad intense fluorescence around ~600 nm.[15,16] By the time-resolved measurements previously preformed by our femtosecond fluorescence up-conversion microscope, the sequential decay in these exciton states was clearly time-resolved at room temperature.[10]

For the femtosecond fluorescence dynamics imaging, the intensity of the up-converted fluorescence was sampled at several delay times and then the ultrafast dynamics was extracted. In the case of α-perylene, the up-converted intensity at three different delay times, −5, 1, and 3 ps, was measured. These delay times were chosen because the ultrafast fluorescence decay of the free exciton is mainly observed in this time region.[10] Figure 3b shows the femtosecond fluorescence dynamics image obtained from the region that is indicated by a broken rectangle in Figure 3a. Figure 3c shows a corresponding contour plot of Figure 3b. The up-conversion measurement was carried out for the fluorescence at 530 nm because of the high intensity of the time-resolved fluorescence at this wavelength, and the up-converted fluorescence data were recorded every 1 μm. It should be mentioned that the α-perylene microcrystals show almost

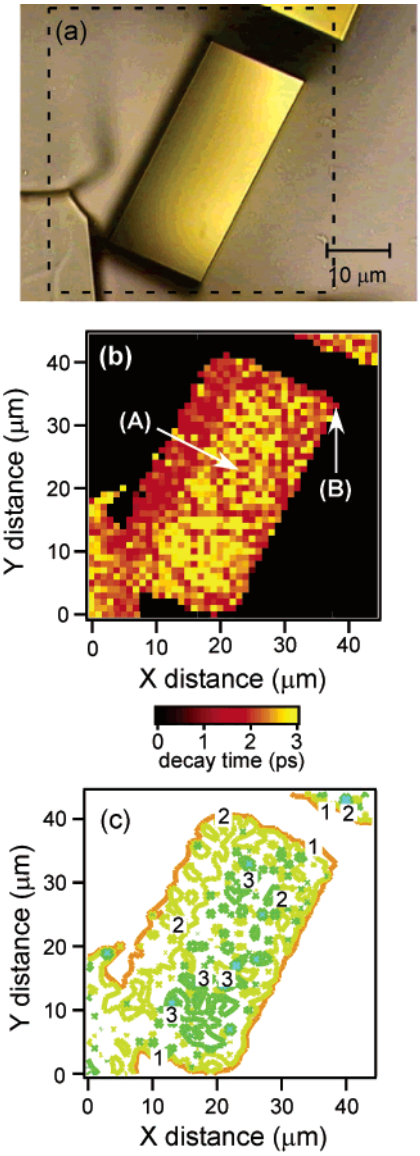

Figure 3. (a) The CCD camera image of the α-perylene microcrystal used for the femtosecond fluorescence dynamics imaging microscopy. (b) The dynamics image obtained from the region indicated by a broken rectangle in part a (excitation 400 nm; fluorescence 530 nm). The time-resolved fluorescence intensity was sampled at the delay times of −5, 1, and 3 ps and the evaluated mean decay time constant was used for the construction of the image. (c) The contour plot of the femtosecond fluorescence dynamics image.

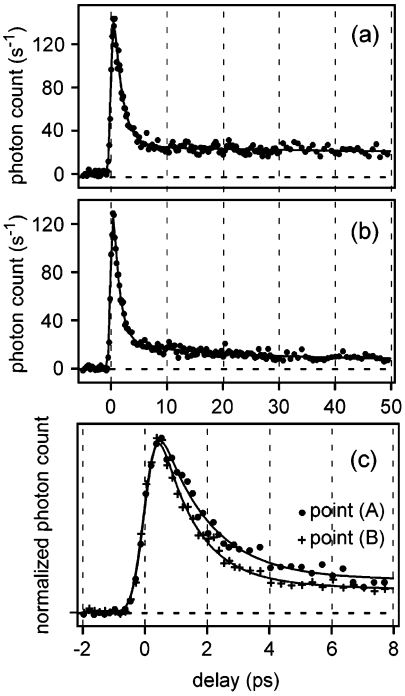

Figure 4. (a) Femtosecond time-resolved fluorescence obtained from the α-perylene microcrystal at the crystal position A in Figure 3b (excitation 400 nm; fluorescence 530 nm). The observed data were well fitted by a triple-exponential function with the time constants of $\tau_1 = 1.5$ ps, $\tau_2 = 38.2$ ps, and $\tau_3 \sim$ long. (b) Femtosecond time-resolved fluorescence obtained at the crystal position B in Figure 3b (excitation 400 nm; fluorescence 530 nm). The observed data were also fitted by a triple-exponential function, and the time constants of $\tau_1 = 1.2$ ps, $\tau_2 = 19.4$ ps, and $\tau_3 \sim$ long were evaluated. (c) Femtosecond time-resolved fluorescence (a) and (b) were expanded for the delay time region from −2 to 8 ps.

no absorption at 530 nm[17] and that the self-absorption for the observed fluorescence can be neglected. In Figure 3b,c, we see most parts of the microcrystal have the mean decay time of 2−3 ps. Our imaging microscope apparatus enables us to go back to a specific sample point and to remeasure a time-resolved fluorescence trace in the whole delay time region. Figure 4a shows the time-resolved fluorescence trace observed at one of the points that showed the mean decay time of 2−3 ps (point A in Figure 3b). The observed data were well fitted by the triple exponential function that is convoluted with the instrumental response. The first two time constants were determined to be $\tau_1 = 1.5$ ps and $\tau_2 = 38.2$ ps, whereas the accurate determination of the third time constant was difficult owing to its very long lifetime ($\tau_3 > 1$ ns). The obtained time constants accord well with the values reported in our previous paper[10] although the τ_1 value was slightly shorter. These three time constants can be assigned to the lifetime of the free exciton, the Y-state, and the E-state. As mentioned, in the previous paper,[10] the observed dynamics was not affected by the change of pulse energy of the excitation. Therefore, the exciton−exciton annihilation was negligible in the excitation energy range in the present experiments. Note that the mean decay time constant derived from the dynamics imaging measurement is longer than the real lifetime of the free exciton. It is because the time-resolved fluorescence in the sampled delay time region is not a single exponential decay but it also includes contribution from the Y- and E-states fluorescence that have relatively long lifetimes. In addition to the sample points that show the mean decay time of 2−3 ps, we also see that the crystal edges showed a short mean decay time of ∼1 ps. The time-resolved fluorescence trace measured at one of these points (point B in Figure 3b) is depicted in Figure 4b. The observed decay was also fitted with the three-exponential function. The lifetime of the free exciton τ_1 was slightly reduced to 1.2 ps and the lifetime of the Y-state τ_2 was also reduced to 19.4 ps. The time-resolved fluorescence data observed at both sample points (point A and B in Figure 3b) in the delay time region from −2 to 8 ps were expanded in Figure 4c. This lifetime shortening of τ_1 and τ_2 components at the crystal edge was also observed in our previous measurement,[10] and it arises from the higher concentration of the crystal defects at the crystal edge. This experiment demonstrated that it is possible to visualize spatial distribution of the defect in an α-perylene microcrystal based on the mean fluorescence decay time in the picosecond/femtosecond time region.

3.2. Tetracene-Doped Anthracene Microcrystal (energy transfer dynamics). Femtosecond fluorescence dynamics imaging was also carried out to visualize the energy transfer dynamics

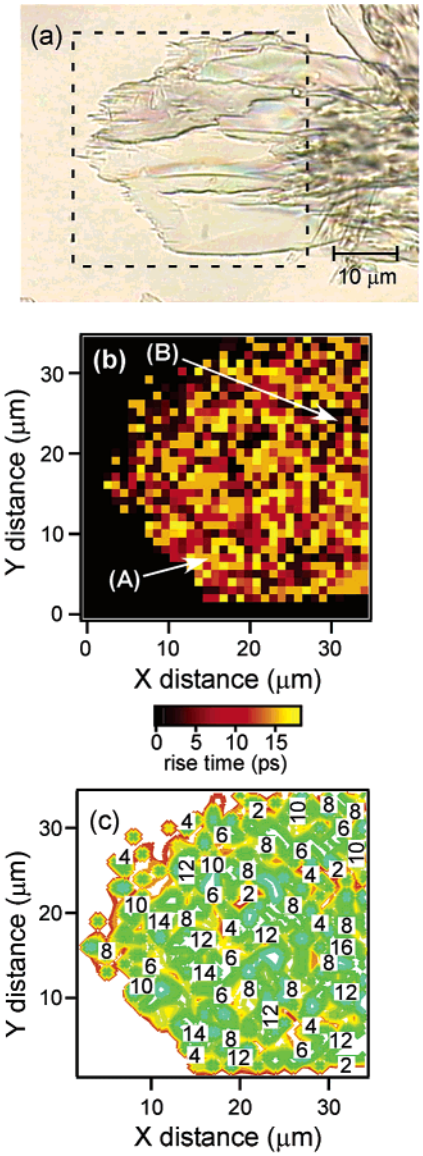

Figure 5. (a) The CCD camera image of the tetracene-doped anthracene microcrystal used for the femtosecond fluorescence dynamics imaging microscopy. (b) The dynamics image obtained from the region indicated by a broken rectangle in part a (excitation 400 nm; fluorescence 530 nm). The time-resolved fluorescence intensity was sampled at the delay times of −5, 5, 15, and 30 ps, and the evaluated mean rise time constant was used for the construction of the image. (c) The contour plot of the femtosecond fluorescence dynamics image.

in a tetracene-doped anthracene microcrystal (mixed microcrystal). The tetracene-doped anthracene microcrystals were recrystallized from the benzene solution of anthracene and tetracene[18] with a molar ratio of 1:0.01 (Figure 5a). By photoexcitation with 400-nm light, this microcrystal exhibited an intense fluorescence spectrum showing vibrational structure at 500, 530, 570, and 620 nm. This fluorescence feature is very similar to that from tetracene in solution, although the peak wavelengths of mixed microcrystal are red shifted by ∼50 nm.[19] Besides, the fluorescence spectrum shows a very good mirror image to the absorption spectrum of tetracene in solution. Therefore, the intense fluorescence observed from the mixed microcrystal was assigned to the fluorescence from a tetracene molecule (monomer) embedded in the anthracene crystal.[20]

Figure 6a depicts the time-resolved fluorescence at 530 nm obtained from the mixed microcrystal. The observed data were well fitted by a single-exponential function that was convoluted

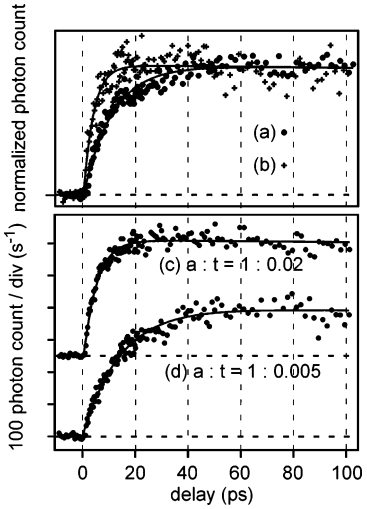

Figure 6. (Upper panel) Femtosecond time-resolved fluorescence obtained from the tetracene-doped anthracene microcrystal at the crystal position A (a) and B (b) in Figure 5b (excitation 400 nm; fluorescence 530 nm). The fluorescence rise representing the excitation energy transfer from anthracene to tetracene was fitted by the single-exponential function, and the rise time constants were evaluated to be 11.1 (a) and 3.9 ps (b). (Lower panel) The time-resolved fluorescence (530 nm) obtained from the tetracene-doped anthracene microcrystal having different molar ratios: anthracene:tetracene = 1:0.02 (c) and 1:0.005 (d). The evaluated rise time constants were 5.0 (c) and 14.8 ps (d).

with the instrumental response. The time constant for the fluorescence rise was determined to be 11.1 ps. The time-resolved fluorescence measurements were also carried out at other intensity maxima of 500, 570, and 620 nm, and the same temporal change of the up-converted fluorescence was observed. Since the tetracene molecule (monomer) and the anthracene crystal have no absorption in the wavelength region longer than 500 nm, the self-absorption effect on the observed fluorescence dynamics can be neglected. Furthermore, we observed the fluorescence *decay* having the same time constant at the blue edge of the steady-state fluorescence spectrum (470 nm), where the fluorescence from anthracene is observed. Therefore, it is obvious that the fluorescence rise depicted in Figure 6a represents the excitation energy transfer from anthracene to a tetracene molecule. Previously, picosecond near-field fluorescence microscopy was performed for the evaporated anthracene−tetracene film by Masuhara and co-workers,[20] and the time-resolved fluorescence data at the wavelengths of 450 and 550 nm were reported. They revealed the fluorescence decay of anthracene and tetracene in the nanosecond time region. However, they could not observe the rise component of tetracene fluorescence. By using the femtosecond fluorescence up-conversion microscope, the rise component of tetracene fluorescence was clearly time-resolved in the present measurement, as shown in Figure 6a.

The fluorescence dynamics imaging was carried out by monitoring time-resolved fluorescence at 530 nm where the rise of the tetracene fluorescence is observed. The up-converted fluorescence data were recorded every 1 μm. The intensity of the up-converted fluorescence was sampled at four delay times of −5, 5, 15, and 30 ps. Because of the single-exponential rise property of the tetracene fluorescence, the evaluated mean time constant τ is identical with the real fluorescence rise time (the energy transfer time). The measurement was carried out for the region indicated by a broken rectangle in Figure 5a and the dynamics image obtained was depicted in Figure 5b. Figure 5c shows a corresponding contour plot of Figure 5b. As seen in this image, the rise time having 10−15 ps was observed in most

parts of the microcrystal. However, we could also see peculiar points at which the rise time was very short. The femtosecond time-resolved fluorescence trace measured at one of these short lifetime points (point B in Figure 5b) is shown in Figure 6b. The observed data were well fitted by a single-exponential function, and the time constant for the fluorescence rise was determined to be 3.9 ps. This time constant is much shorter than the typical value derived from the crystal point (A) in Figure 5b. (The data obtained from point A are shown in Figure 6a.) Although we could not recognize a noticeable difference between the steady-state fluorescence spectra measured at two different specific points, it is clear that the inhomogeneity in the mixed microcrystal affects the dynamics of the excitation energy transfer from anthracene to tetracene. The mixed microcrystal was prepared by the evaporation of solvent on a cover glass, so that it is expected that the tetracene molecule is inhomogeneously distributed in the microcrystal. Therefore, it is highly likely that the difference in the rise time arises from the difference in the local concentration of tetracene. This argument was strongly confirmed by the following experiment. We made two types of tetracene-doped anthracene microcrystal in which the molar ratios between the anthracene and the tetracene were 1:0.02 and 1:0.005 and measured the femtosecond fluorescence dynamics images from both microcrystals. Then, we measured time-resolved fluorescence traces, selecting the positions that show typical fluorescence rise times. As shown in Figure 6c,d, the time constant for the excitation energy transfer from the anthracene to tetracene was affected by the tetracene concentration, and the lifetime was determined to be 5.0 (1:0.02) and 14.8 ps (1:0.005), respectively. Therefore, it is safely concluded that the crystal point B is the point where the tetracene concentration is high. This implies that the fluorescence dynamics image obtained successfully represents the difference in local concentration of the tetracene molecule in the mixed microcrystal.

4. Conclusion

The femtosecond fluorescence dynamics imaging was carried out using the fluorescence up-conversion microscope in order to visualize position-dependent ultrafast fluorescence dynamics in organic microcrystals, α-perylene and tetracene-doped anthracene. The ultrafast fluorescence dynamics images were constructed on the basis of the mean fluorescence decay or rise time constants, which were evaluated by the intensity sampling of time-resolved fluorescence at selected delay times. Taking advantage of femtosecond time and diffraction-limit space resolution, ultrafast dynamics in the organic microcrystals were clearly imaged in the two-dimensional manner. For the α-perylene microcrystal, the obtained dynamics images clearly showed that the crystal edges have relatively shorter free exciton and the Y-state lifetimes compared to the crystal center, reflecting a high concentration of defects in the edges. For the tetracene-doped anthracene microcrystal, the dynamics image was constructed based on the time constant of excitation energy transfer from anthracene to tetracene. By the experiments with changing doping ratios of tetracene in anthracene, it was found that the inhomogeneity observed in the dynamics image is attributed to the difference in the local concentration of tetracene. We consider that this type of dynamics imaging microscopy can be a powerful method in visualizing the material based on the ultrafast dynamics.

Acknowledgment. Tatsuya Fujino and Takuya Fujima acknowledge the Special Postdoctral Researchers Program of RIKEN. Tatsuya Fujino acknowledges a Grant-in-Aid for Young Scientists (A) from Japan Society for Promotion of Science (No. 17685004).

References and Notes

(1) de Grauw, C. J.; Gerritsen, H. C. *Appl. Spectrosc.* **2001**, *55*, 670.
(2) Sytsma, J.; Vroom, J. M.; Graum, C. J. D.; Gerritsen, H. C. *J. Microsc.* **1998**, *191*, 39.
(3) Duncan, R. R.; Bergmann, A.; Cousin, M. A.; Apps, D. K.; Shipston, M. J. *J. Microsc.* **2004**, *215*, 1.
(4) Li, Q. A.; Ruckstuhl, T.; Seeger, S. *J. Phys. Chem. B* **2004**, *108*, 8324.
(5) Emiliani, V.; Sanvitto, D.; Tramier, M.; Piolot, T.; Petrasek, Z.; Kemnitz, K.; Durieux, C.; Coppey-Moisan, M. *Appl. Phys. Lett.* **2003**, *83*, 2471.
(6) Tinnefeld, P.; Herten, D. P.; Sauer, M. *J. Phys. Chem. A* **2001**, *105*, 7989.
(7) Periasamy, A.; Wodnicki, P.; Wang, X. F.; Kwon, S.; Gordon, G. W.; Herman, B. *Rev. Sci. Instrum.* **1996**, *67*, 3722.
(8) Krishnan, R. V.; Biener, E.; Zhang, J. H.; Heckel, R.; Herman, B. *Appl. Phys. Lett.* **2003**, *83*, 4658.
(9) Krishnan, R. V.; Saitoh, H.; Terada, H.; Centonze, V. E.; Herman, B. *Rev. Sci. Instrum.* **2003**, *74*, 2714.
(10) Fujino, T.; Tahara, T. *J. Phys. Chem. B* **2003**, *107*, 5120.
(11) Fujino, T.; Tahara, T. *Appl. Phys. B* **2004**, *79*, 145.
(12) Shah, J. *IEEE J. Quantum Electron.* **1988**, *24*, 276.
(13) Takeuchi, S.; Tahara, T. *J. Phys. Chem. A* **1998**, *102*, 7740.
(14) Tamai, N.; Porter, C. F.; Masuhara, H. *Chem. Phys. Lett.* **1993**, *211*, 364.
(15) Auweter, H.; Ramer, D.; Kunze, B.; Wolf, H. C. *Chem. Phys. Lett.* **1982**, *85*, 325.
(16) Nishimura, H.; Yamaoka, T.; Mizuno, K.; Iemura, M.; Matsui, A. *J. Phys. Soc. Jpn.* **1984**, *53*, 3999.
(17) Fuke, K.; Kaya, K.; Kajiwara, T.; Nagakura, S. *J. Mol. Spectrosc.* **1976**, *63*, 98.
(18) Huppert, D.; Rojansky, D. *Chem. Phys. Lett.* **1985**, *114*, 149.
(19) Sarkar, N.; Takeuchi, S.; Tahara, T. *J. Phys. Chem. A* **1999**, *103*, 4808.
(20) Yoshikawa, H.; Sasaki, K.; Masuhara, H. *J. Phys. Chem. B* **2000**, *104*, 3429.